


Molecular heterogeneity in aqueous cosolvent systems ^F

Cite as: J. Chem. Phys. **152**, 190901 (2020); <https://doi.org/10.1063/5.0007647>

Submitted: 16 March 2020 • Accepted: 24 April 2020 • Published Online: 18 May 2020

Kwang-Im Oh and  Carlos R. Baiz

COLLECTIONS

 This paper was selected as Featured



View Online



Export Citation



CrossMark

ARTICLES YOU MAY BE INTERESTED IN

[Simulations of activities, solubilities, transport properties, and nucleation rates for aqueous electrolyte solutions](#)

The Journal of Chemical Physics **153**, 010903 (2020); <https://doi.org/10.1063/5.0012102>

[Toward empirical force fields that match experimental observables](#)

The Journal of Chemical Physics **152**, 230902 (2020); <https://doi.org/10.1063/5.0011346>

[Essentials of relativistic quantum chemistry](#)

The Journal of Chemical Physics **152**, 180901 (2020); <https://doi.org/10.1063/5.0008432>

Lock-in Amplifiers
up to 600 MHz



Zurich
Instruments



Molecular heterogeneity in aqueous cosolvent systems

Cite as: J. Chem. Phys. 152, 190901 (2020); doi: 10.1063/5.0007647

Submitted: 16 March 2020 • Accepted: 24 April 2020 •

Published Online: 18 May 2020



View Online



Export Citation



CrossMark

Kwang-Im Oh and Carlos R. Baiz^{a)} 

AFFILIATIONS

Department of Chemistry, University of Texas at Austin, Austin, Texas 19104, USA

^{a)} Author to whom correspondence should be addressed: cbaiz@cm.utexas.edu

ABSTRACT

Aqueous cosolvent systems (ACoSs) are mixtures of small polar molecules such as amides, alcohols, dimethyl sulfoxide, or ions in water. These liquids have been the focus of fundamental studies due to their complex intermolecular interactions as well as their broad applications in chemistry, medicine, and materials science. ACoSs are fully miscible at the macroscopic level but exhibit nanometer-scale spatial heterogeneity. ACoSs have recently received renewed attention within the chemical physics community as model systems to explore the relationship between intermolecular interactions and microscopic liquid–liquid phase separation. In this perspective, we provide an overview of ACoS spatial segregation, dynamic heterogeneity, and multiscale relaxation dynamics. We describe emerging approaches to characterize liquid microstructure, H-bond networks, and dynamics using modern experimental tools combined with molecular dynamics simulations and network-based analysis techniques.

Published under license by AIP Publishing. <https://doi.org/10.1063/5.0007647>

I. INTRODUCTION

Aqueous cosolvent systems (ACoSs) are binary mixtures composed of small, polar organic molecules, such as alcohols, dimethyl sulfoxide, or amides in water. ACoSs exhibit composition-dependent bulk properties that deviate significantly from the ideal behavior as a result of microscopic heterogeneity and liquid–liquid phase separation.^{1–10} These properties are often exploited in chemical synthesis where solubility and reaction kinetics can be modulated by tuning ACoS composition.^{10,11} In recent years, ACoSs have received renewed attention because heterogeneous binary liquids are minimal model systems for understanding spontaneous assembly in multicomponent biological systems, in particular, since phase separation results from a subtle balance of intermolecular interactions across different components. Specifically, subcellular cytosolic compartments enriched in certain proteins or nucleic acids, known as “membraneless organelles,” can be considered a complex example of liquid–liquid phase separation.^{12–14}

Similarly, concentrated aqueous electrolyte solutions have recently received attention within the physical chemistry community because these solutions exhibit partial phase separation. Part of this renewed interest in ionic compounds also arises from their

potential for use in next-generation water-based electrolytes for lithium-ion or zinc batteries.^{15–18} Ionic compounds are not “cosolvents”; however, the complex properties of ionic solutions mirror those of organic ACoSs. The majority of this perspective is focused on organic ACoSs, but we also discuss ionic compounds as a point of comparison to highlight important parallels between the two systems.

II. MICROSCOPIC HETEROGENEITY

Spatial heterogeneity can be understood in terms of non-uniform composition gradients; microscopic phase separation describes the limit in which each component remains separated by a well-defined interface. [Figure 1\(a\)](#) shows the clustered microstructure of a DMSO–water system. Disrupted H-bonds are present near the interface between two regions, and bulk-like tetrahedral H-bond structures are observed in water-rich regions. Heterogeneity results from the subtle balance between water–water, water–cosolvent, and cosolvent–cosolvent intermolecular forces. Given the noncovalent nature of these interactions, quantitatively describing ACoS heterogeneity remains challenging.

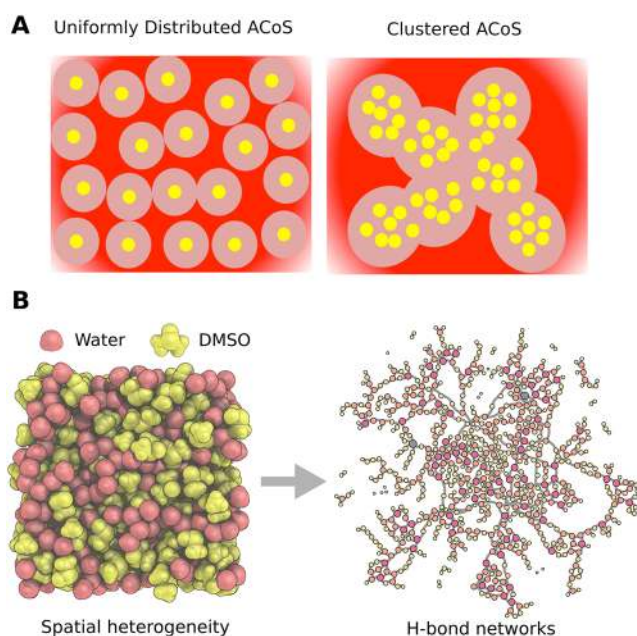


FIG. 1. (a) Illustration of uniformly distributed (left) and clustered (right) aqueous cosolvent systems (ACoSs). Yellow and red represent amphiphilic molecules of ions and water, respectively. Light red circles indicate interfacial regions with disrupted H-bonds. (b) Example of molecular distribution (left) and H-bond networks (right) of a heterogeneous DMSO–water mixture generated from an MD snapshot. The nodes represent water molecules, and the edges represent H-bonds. Reprinted with permission from Oh *et al.*, *J. Phys. Chem. Lett.* **11**, 1903 (2020). Copyright 2020 American Chemical Society.

Molecular dynamics (MD) simulations provide the most complete description of a liquid: the exact positions of all atoms as a function of time are represented in each trajectory. However, quantifying the microscopic liquid structure, nevertheless, requires novel analysis tools because traditional methods, such as pair correlation functions, often fail to provide insights into the microstructure of heterogeneous liquids. Network-based analysis tools have recently been applied to ACoS simulations.¹⁹ Within these models, H-bonded or spatially colocalized molecules are considered to be “connected” to each other in the network. Analysis algorithms can be applied to describe the topology of the network, which can then describe the extended structure and interactions within the liquids [Fig. 1(b)].^{20–29}

One could argue that ACoS descriptions derived from MD simulations are highly dependent on the choice of force field because intermolecular interactions are difficult to model with classical MD.^{30,31} Nonetheless, microheterogeneity is observed using a variety of force fields.^{19,29,32,33} Specific liquid morphologies may be model dependent, but phase separation itself is readily captured with relatively simple united-atom models.³⁴ For instance, Perera and co-workers reported aggregate structures in alcohol–water,^{32,35} DMSO–water,²⁹ and other ACoSs using a variety of force fields and methods.^{29,32,35–40} Similarly, in ionic solutions, despite strong electrostatic interactions, cluster morphologies emerge from a combination of electrolyte properties.^{25,41–44} Mason and co-workers investigated

the differences between guanidinium sulfate and guanidinium thiocyanate using neutron diffraction and MD simulations and showed that only sulfate leads to phase separation.^{45,46} Similarly, Cho and co-workers used ultrafast spectroscopy together with MD simulations to show that chaotropic anions build ion networks intertwined with water networks, while kosmotropic anions form quasi-crystalline ion clusters.^{47–51} These examples showcase the powerful combination of molecular spectroscopy and simulations: Experiments are used to benchmark force fields ensuring that the MD produces an accurate description of the microscopic ensembles, and then, trajectories are analyzed to link specific molecular interactions with solvent properties of interest.^{39,52–55}

Liquid microstructure is perhaps one defining aspect of ACoSs; however, the evolving environments within the liquid are significantly more challenging to characterize. Dynamics in ACoSs span several timescales, and therefore, the measured relaxation rates are highly dependent on the experimental technique as well as the experimental probe employed. Even within the same ACoSs, different measurements capture different dynamics.^{18,21,55–72} For example, ultrafast spectroscopy on vibrational probes reports on the fast H-bond exchange.^{19,57–61,72–74} Time-resolved fluorescence measurements report on solvation dynamics as well as the molecular reorientation probe itself.^{19,74,76,77} Measured lifetimes are interpreted in terms of the local solvation environment around the probe, which is sometimes modeled using MD simulations.⁶⁵ The relationship between molecular interactions, phase separation, and local dynamics is unique to each system. In DMSO–water ACoSs, for example, picosecond dynamics are fastest around 35 mol. % DMSO, which coincides with the highest positive deviation in density, suggesting that bulk properties, such as average molecular packing efficiency, provide incomplete descriptions of the molecular interactions in ACoSs.^{5,19}

In this perspective, we present an overview of the current understanding of ACoSs and provide an outlook focused on major obstacles that must be overcome to achieve a comprehensive description that links molecular interactions to microscopic heterogeneity in these complex liquids.

III. INTERMOLECULAR INTERACTIONS

Thermodynamics provides the most fundamental descriptions of ACoSs. Liquid heterogeneity, dynamics, and bulk properties of ACoSs are fundamentally determined by intermolecular interactions among different components. Initial ACoS studies focused on bulk thermodynamics, including excess enthalpies or entropies of mixing or excess volume, to describe the deviations from ideality. These quantities are useful because they can be directly computed from pair correlation functions via Kirkwood–Buff integrals.^{29,32,35–37,39,40} Such bulk quantities provide limited insight into the microstructure and intermolecular interactions in the liquids yet are nonetheless useful benchmarks for models and simulations.^{32,37,39,75}

A. H-bond energies and configurations

Significant efforts have been dedicated to accurately modeling H-bond interactions. Energies and configurations have been computed using a wide repertoire of electronic structure methods.^{76–81} Experimentally determining H-bond thermodynamics remains

difficult as H-bond making/breaking involves reorganization of the extended network, and as a result, measured enthalpies are highly composition-dependent. In this section, we provide examples of commonly studied systems to illustrate key challenges associated with characterizing H-bonding in ACoSs.

Water contains an equal number of H-bond donors and acceptors, forming an approximately tetrahedral H-bond network.⁸² Within low cosolvent concentrations, the donor/acceptor balance and the tetrahedral structures are largely preserved. Higher cosolvent concentrations alter this donor/acceptor balance, resulting in unoccupied H-bond sites. H-bond populations are therefore highly composition dependent.^{32,35–38,42–44,46,83,84} For example, DMSO can accept two H-bonds through its oxygen lone pairs; however, DMSO–DMSO non-polar interactions contribute to molecular segregation, producing a mosaic of H-bonding environments.^{1,65,85} H-bond networks are largely preserved in the water-rich regions despite the overall donor/acceptor imbalance.^{76–78} MD simulations suggest stable 1-DMSO:2-water structures in dilute DMSO solutions and stable 2-DMSO:1-water species in the DMSO-rich (>50 mol. %) regime.^{76–78} Bagchi and co-workers suggested the presence of percolating water networks in aqueous DMSO solutions.^{65,86–88} Oh *et al.* proposed the “step in” mechanism involving two species to describe the H-bond forming and breaking mechanism in DMSO–water mixtures.⁸⁹ These examples highlight the complexity of H-bond making/breaking mechanisms in heterogeneous solutions.

Alcohols have been widely studied due to their importance in chemical and industrial applications. Alcohol–water ACoS heterogeneity, in particular, has been characterized using neutron diffraction, vibrational spectroscopy, and an array of MD simulations.^{1,9,21,41,84,90} Nishi *et al.* proposed the presence of a distinct $(C_2H_5OH)_m(H_2O)_n$ species whose composition varied significantly with the ethanol mole ratio.^{91,92} Another challenging cosolvent is tert-butyl alcohol. Kusalik *et al.* found phase separation in concentrations as low as 8 mol. %.⁹¹ Elber and co-workers showed that minor alterations to the Lennard-Jones coefficients improve the accuracy of the predicted bulk liquid properties.³⁴ These studies, once again, show that phase separation is the result of a subtle balance between the interaction potentials for different species. Another interesting polar molecule *N*-methyl acetamide (NMA) has received significant attention, particularly within the ultrafast community, as a minimal amino-acid model.⁹³ Recently, Pshenichnikov

and co-workers showed that hydrophobic interactions between methyl groups in aqueous NMA induce clustering,⁹⁴ suggesting that the protein backbone may contribute significantly to folding through hydrophobic collapse and self H-bond interactions.

Comparing composition-dependent H-bond populations across different cosolvents is a common approach to connect intermolecular interactions, heterogeneity, and H-bonding environments.^{36,37,53,74,95–97} While this approach appears useful at the first glance, replacing even one atom alters the cosolvent properties and therefore produces widely different ACoS environments; thus, comparative studies often fail to produce fundamental insights. For example, acetone differs from DMSO by only one atom, but replacing S with C alters the molecular geometry from planar to non-planar and lowers the dipole moment strength (2.91 D and 3.96 D for acetone and DMSO, respectively).^{98,99} Water–acetone H-bond enthalpies (~20 kJ/mol) are significantly weaker than DMSO–water enthalpies (~60 kJ/mol).^{95,100} Within a comparative approach, MD simulations have one important advantage: molecular properties such as atomic charges and Van der Waals radii can be controlled independently of molecular geometries. Indeed, force field comparisons are useful in understanding the relation between intermolecular interactions and phase separation.^{36,37,53,74,95–97}

B. Extended H-bond structures

The specific mechanisms by which the cosolvent perturbs the H-bond networks and, more importantly, the role of H-bonding in microscopic segregation are not completely understood.^{1,34,53,95–97} The need to achieve a mechanistic picture has recently driven the development of quantitative methods based on models adopted from graph theory. These mathematical tools are ideally suited to describing cosolvent effects on H-bond network topologies.^{47–51,103,104} Within this approach, a given H-bond network is described as an adjacency matrix representing vertices (molecules) and edges (H-bonds). In water, each molecule can make up to four H-bonds although 5-bond configurations are observed transiently.³⁰ An example of an H-bond network in a DMSO–water ACoS is shown in Fig. 1(b). Eigenvectors of the matrix represent the instantaneous size of the networks.¹⁹ Cho and co-workers recently developed mathematical tools to characterize aggregation in aqueous electrolytes.^{50,105,106} Simulations predict ion clusters within the

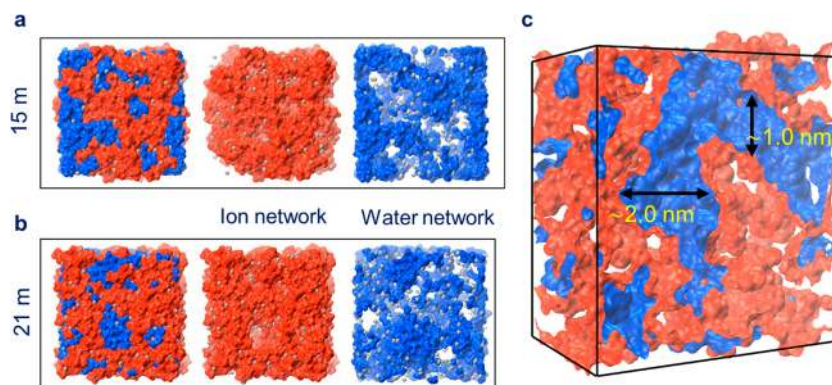


FIG. 2. Snapshots of MD simulation trajectories showing water channels in an electrolyte solution. Reprinted with permission from Lim *et al.*, *J. Am. Chem. Soc.* **140**, 15661 (2018), Copyright 2018 American Chemical Society.

water H-bond network, and, most interestingly, the formation of nanometer-scale water “channels” (Fig. 2).¹⁸ Network models have recently offered a fresh perspective of DMSO–water ACoSs. Clusters of ~25 water molecules are observed at 30 mol.% DMSO, suggesting that heterogeneity occurs on the nm length scale.¹⁹ H-bond networks display hub-and-spoke topologies consisting of a central cluster surrounded by smaller “wire-like” networks that are only connected to the main hub by a few H-bonds [Fig. 1(b)]. These are two examples of heterogeneity on the nanometer length scale. The rapid reorganization of the clusters along with their nanometer size makes it particularly challenging to experimentally verify these predictions; nonetheless, experiments are generally consistent with heterogeneity on the above-mentioned length scales.

Geometric order parameters are commonly used to describe local ordering in water. Most notably, Debenedetti and co-workers¹⁰⁷ have constructed a tetrahedral order parameter (q) that considers the angles between a central water molecule and its four nearest neighbors. This parameter takes on a value of 1 for the perfectly tetrahedral structure of ice and 0 for an ensemble of random configurations (i.e., an ideal gas). The translational order parameter, S_k , considers variation in distances between a central water and its four nearest neighbors.¹⁰⁸ Likewise, the parameter takes on a value of 1 for a perfectly ordered tetrahedral configuration with identical distances between a central water and its four nearest neighbors. Despite both parameters measuring similar characteristics, the Pearson correlation between these two order parameters is only 0.26. In fact, among six order parameters examined by Laage and co-workers (Fig. 3), the highest Pearson correlation among any pair is 0.52, suggesting that quantitative descriptions are highly subject to the definition used.¹⁰⁹ Through their comparison, the authors suggested that the asphericity and tetrahedral order parameters are most sensitive to local structural fluctuations around hydrophobic molecules. To our knowledge, systematic order parameter comparisons within ACoS simulations have not been carried out; nonetheless, the tetrahedral order parameter has been useful in quantifying local structural fluctuations in DMSO–water ACoS simulations.¹⁹

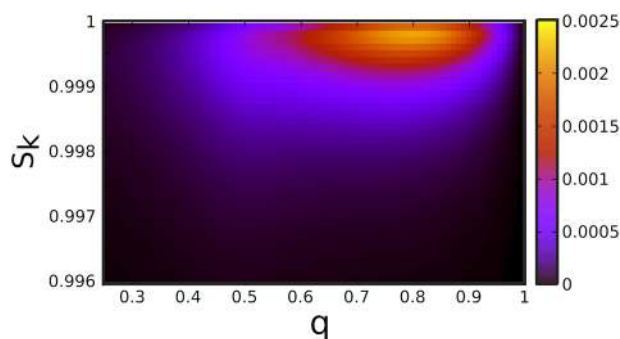


FIG. 3. Joint probability distributions showing the correlation between the tetrahedral order parameter (q) and the asphericity parameter (S_k) of water. Adapted with permission from E. Duboué-Dijon and D. Laage, *J. Phys. Chem. B* **119**, 8406 (2015). Copyright 2018 American Chemical Society.

IV. MD SIMULATIONS

Experiments and simulations often go hand-in-hand: experiments are used to benchmark models, and, in turn, trajectories assist in interpreting experiments, providing an atomistic view of ACoS phase separation and serving as a platform to test hypotheses and design future experiments.^{110,111}

A. Interaction potentials

Selecting suitable MD potentials remains a significant challenge.^{111–116} Reparameterizing force fields to reproduce specific experimental measurements is common.^{41,117–119} For instance, Soetens and Bopp showed that optimizing water and methanol force field parameters reproduces key macroscopic properties, such as density and partial molar volumes, over the entire composition region.¹²⁰ Popular water models such as SPC/E, TIP4P, and TIP4P-Ew combined with OPLS-AA have also been useful for modeling alcohols.^{31,38,103,110,121–123} Electrolytes remain a greater challenge because ion–ion interactions are increasingly difficult to model. Potentials generally overestimate attractive interactions, leading to artificial aggregation of charged species.^{62,105,106,124–126} Pair-specific corrections to the Lennard-Jones potentials for cations have increased the accuracy of ion–biomolecule binding affinities,^{124–126} and similar parameter optimizations may also prove useful for electrolytes. In conclusion, significant improvements to potentials and algorithms have been made in recent years, mainly driven by the need to more accurately reproduce bulk measurable quantities, including thermodynamics, density, partial volumes, and viscosity; most recently, these metrics include microstructure-specific measurements such as neutron diffraction patterns and H-bond populations. Future work should focus on developing more general approaches to parameterize several classes of cosolvents or ions at once, avoiding the need to benchmark individual systems against the experiment.

B. Multiscale dynamics

Like biomolecules, ACoS dynamics span several decades in time from picosecond H-bond lifetimes to millisecond bulk reorganization of the liquid, as represented in Fig. 4. This behavior stems from rough free energy landscapes, similar to how proteins undergo hierarchical dynamics when sampling different regions of conformational space.^{127–130} The liquid microstructure emerges from the balance between three types of intermolecular interactions: water–water, water–cosolvent, and cosolvent–cosolvent. Naturally, dynamic reorganization exhibits composition-dependent behavior across timescales. We use the term “dynamic heterogeneity” to describe multiscale relaxation in ACoSs, analogous to glasses and supercooled liquids where heterogeneity produces nonexponential relaxation.¹³¹ Stretched exponentials also describe certain ACoS dynamics,¹³² suggesting a rough potential energy landscape, but, in addition, ACoS dynamics span several timescales, similar to proteins (Fig. 4), indicating a range of peaks and valleys across different energy scales within the landscape.¹³³

Dynamics in ACoSs have been studied extensively with varying success.^{19,57–61,70–74} Two challenging questions have not yet been fully addressed: (1) How does spatial heterogeneity correlate with dynamic heterogeneity? (2) Given that the environment around a

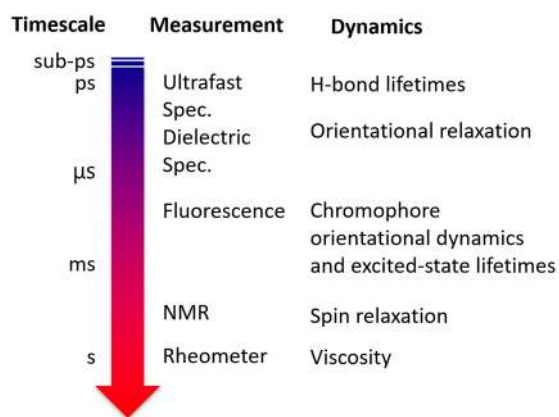


FIG. 4. Schematic diagram of ACoS relaxation timescales probed by different experiments.

molecular probe is composition-dependent, how can one interpret the multiscale motions of the liquids from time-resolved measurements on a local probe? The second question is particularly challenging because different probes report on different dynamics, as dictated by the local environment around the probe.^{19,56–58,64–66,74,134,135} Figure 4 shows a summary of the relaxation timescales measured using different techniques, demonstrating that no single technique can capture the full range of timescales, and as a consequence, a wide repertoire of techniques are required to measure dynamic heterogeneity.^{19,25–28,67–72,74,134–136}

ACoS dynamics are considerably slower than bulk water. Cosolvents perturb the tetrahedral H-bond networks and increase H-bond lifetimes.^{53,62–69,71} In general, solvation dynamics become slowest within equimolar concentrations. For example, in DMSO–water mixtures, the orientational dynamics of a fluorescent probe and nuclear magnetic resonance (NMR) proton spin relaxation both report the slowest dynamics near equimolar concentrations.^{134,137} Observed trends in local dynamics generally agree with the trends in bulk viscosity.^{18,26,83,120,138}

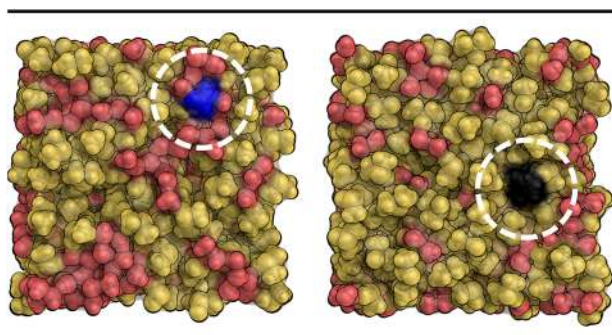


FIG. 5. MD snapshots generated from a DMSO–water MD simulation (trajectories from data in Ref. 30). DMSO is shown in yellow and water in red. Two probes formamide (blue) and dimethylformamide (black) are represented. Formamide is preferentially surrounded by water, while dimethyl formamide is surrounded by DMSO.

Unlike dilute solutions, where the solute experiences a uniform solvent environment, heterogeneity produces a gradient of molecular environments around a dilute probe. The probe may be localized to either of the two liquid phases or the interface. Figure 5 illustrates this phenomenon for two molecular probes: formamide (FA, highly polar) and dimethylformamide (DMF, less polar) in a 30 mol. % DMSO–water ACoS simulation.¹⁹ In this example, FA localizes primarily to the aqueous phase, whereas DMF localizes to the DMSO-rich phase, showing that probe-dependent solvation dynamics may be useful for determining the extent of preferential interactions as well as for characterizing the dynamics within individual phases.

V. SUMMARY AND OUTLOOK

Spatial heterogeneity and multiscale dynamics define the physical properties of aqueous cosolvent systems. These properties deviate significantly from the ideal behavior and may be distinct from the individual components. Within a practical perspective, tailored ACoS compositions have important real-world applications, for example, modulating the kinetics of chemical reactions by orders of magnitude.^{10,11}

In this perspective, we argue that the most powerful approach for understanding the mechanisms of phase separation at the molecular scale is a combination of MD simulations together with time-resolved measurements on different dynamical probes. When properly benchmarked, simulations provide an atom-by-atom view of the liquid structure. While atomistic trajectories provide the ultimate molecular description, defining liquid microstructure and hierarchical dynamics requires sophisticated and nuanced analysis methods.

ACoSs have received renewed attention in recent years because these liquids may serve as model systems for complex phase separation in biological environments. The ACoS field will continue to grow and confront the important challenges outlined here. The current focus remains on binary liquids; we predict that future efforts will explore the physical chemistry of biological phase-separation using large-scale simulations and, ultimately, describe the environments within intracellular compartments, such as membraneless organelles.

ACKNOWLEDGMENTS

We acknowledge generous support from the National Science Foundation (Grant No. CHE-1847199), the National Institutes of Health (Grant No. R35GM133359), and the Welch Foundation (Grant No. F-1891). This is a Plan II SAWIAGOS Project.

DATA AVAILABILITY

Data sharing is not applicable to this article as no new data were created or analyzed in this study.

REFERENCES

- S. Dixit *et al.*, *Nature* **416**, 829 (2002).
- R. F. Lama and B. C.-Y. Lu, *J. Chem. Eng. Data* **10**, 216 (1965).
- J. Catalán, C. Díaz, and F. García-Blanco, *J. Org. Chem.* **66**, 5846 (2001).
- K. Mochizuki, S. R. Pattenaude, and D. Ben-Amotz, *J. Am. Chem. Soc.* **138**, 9045 (2016).

- ⁵D. H. Rasmussen and A. P. MacKenzie, *Nature* **220**, 1315 (1968).
- ⁶W. Liu *et al.*, *J. Mol. Liq.* **140**, 68 (2008).
- ⁷R. Notman *et al.*, *J. Am. Chem. Soc.* **128**, 13982 (2006).
- ⁸J. Rösgen, B. M. Pettitt, and D. W. Bolen, *Biophys. J.* **89**, 2988 (2005).
- ⁹J. J. Towey, A. K. Soper, and L. Dougan, *Faraday Discuss.* **167**, 159 (2013).
- ¹⁰W. Miao and T. H. Chan, *Acc. Chem. Res.* **39**, 897 (2006).
- ¹¹M. C. Pirrung, *Chem. - Eur. J.* **12**, 1312 (2006).
- ¹²S. Boeynaems *et al.*, *Trends Cell Biol.* **28**, 420 (2018).
- ¹³K. K. Nakashima, M. A. Vibhute, and E. Spruijt, *Front. Mol. Biosci.* **6**, 21 (2019).
- ¹⁴V. N. Uversky, *Curr. Opin. Struct. Biol.* **44**, 18 (2017).
- ¹⁵L. Suo *et al.*, *Science* **350**, 938 (2015).
- ¹⁶X. Wang *et al.*, *Sci. Rep.* **3**, 1401 (2013).
- ¹⁷H. Kim *et al.*, *Chem. Rev.* **114**, 11788 (2014).
- ¹⁸J. Lim *et al.*, *J. Am. Chem. Soc.* **140**, 15661 (2018).
- ¹⁹K.-I. Oh *et al.*, *J. Phys. Chem. Lett.* **11**, 1903 (2020).
- ²⁰P. Bordat *et al.*, *Europhys. Lett.* **65**, 41 (2004).
- ²¹S. Chatterjee *et al.*, *J. Phys. Chem. B* **123**, 9355 (2019).
- ²²B. Chen and J. I. Siepmann, *J. Phys. Chem. B* **110**, 3555 (2006).
- ²³C. Corsaro *et al.*, *J. Phys. Chem. B* **112**, 10449 (2008).
- ²⁴M. D'Angelo, G. Onori, and A. Santucci, *J. Chem. Phys.* **100**, 3107 (1994).
- ²⁵A. Duereh *et al.*, *J. Phys. Chem. B* **122**, 10894 (2018).
- ²⁶R. Li *et al.*, *J. Phys. Chem. B* **118**, 10156 (2014).
- ²⁷S. Pothoczki, L. Pusztai, and I. Bakó, *J. Mol. Liq.* **271**, 571 (2018).
- ²⁸R. Sinibaldi *et al.*, *J. Phys. Chem. B* **110**, 8885 (2006).
- ²⁹A. Perera and R. Mazighi, *J. Chem. Phys.* **143**, 154502 (2015).
- ³⁰M.-L. Tan *et al.*, *J. Chem. Phys.* **142**, 064501 (2015).
- ³¹C. Sanchez, H. Dominguez, and O. Pizio, *Condens. Matter Phys.* **22**, 13602 (2019).
- ³²A. Perera and B. Kežić, *Faraday Discuss.* **167**, 145 (2013).
- ³³O. Borodin *et al.*, *ACS Nano* **11**, 10462 (2017).
- ³⁴M. Di Pierro, M. L. Mugnai, and R. Elber, *J. Phys. Chem. B* **119**, 836 (2015).
- ³⁵B. Kežić and A. Perera, *J. Chem. Phys.* **137**, 014501 (2012).
- ³⁶B. Kežić and A. Perera, *J. Chem. Phys.* **137**, 134502 (2012).
- ³⁷A. Perera and F. Sokolić, *J. Chem. Phys.* **121**, 11272 (2004).
- ³⁸L. Almásy *et al.*, *Phys. Chem. Chem. Phys.* **21**, 9317 (2019).
- ³⁹L. Zoranić *et al.*, *J. Phys. Chem. C* **111**, 15586 (2007).
- ⁴⁰L. Zoranić *et al.*, *J. Chem. Phys.* **130**, 124315 (2009).
- ⁴¹M. Nagasaka *et al.*, *J. Phys. Chem. B* **118**, 4388 (2014).
- ⁴²J. L. Dashnau *et al.*, *J. Phys. Chem. B* **110**, 13670 (2006).
- ⁴³M. Ferrario *et al.*, *J. Chem. Phys.* **93**, 5156 (1990).
- ⁴⁴S. Daschakraborty, *J. Chem. Phys.* **148**, 134501 (2018).
- ⁴⁵P. E. Mason *et al.*, *J. Am. Chem. Soc.* **126**, 11462 (2004).
- ⁴⁶P. E. Mason *et al.*, *J. Phys. Chem. B* **109**, 24185 (2005).
- ⁴⁷J.-H. Choi and M. Cho, *J. Chem. Phys.* **141**, 154502 (2014).
- ⁴⁸J.-H. Choi and M. Cho, *J. Chem. Phys.* **143**, 104110 (2015).
- ⁴⁹J.-H. Choi *et al.*, *J. Chem. Phys.* **142**, 204102 (2015).
- ⁵⁰J.-H. Choi *et al.*, *Annu. Rev. Phys. Chem.* **69**, 125 (2018).
- ⁵¹S. Kim *et al.*, *J. Chem. Phys.* **141**, 124510 (2014).
- ⁵²I. Bakó *et al.*, *J. Chem. Phys.* **132**, 014506 (2010).
- ⁵³S. E. McLain, A. K. Soper, and A. Luzar, *J. Chem. Phys.* **127**, 174515 (2007).
- ⁵⁴D. Subramanian *et al.*, *Faraday Discuss.* **167**, 217 (2014).
- ⁵⁵A. A. Bakulin *et al.*, *Acc. Chem. Res.* **42**, 1229 (2009).
- ⁵⁶A. A. Bakulin *et al.*, *J. Phys. Chem. A* **115**, 1821 (2011).
- ⁵⁷D. Banik *et al.*, *J. Chem. Phys.* **142**, 054505 (2015).
- ⁵⁸D. Banik *et al.*, *J. Phys. Chem. B* **119**, 9905 (2015).
- ⁵⁹M. K. Hazra and B. Bagchi, *J. Chem. Phys.* **148**, 114506 (2018).
- ⁶⁰S. M. Kashid *et al.*, *J. Phys. Chem. B* **119**, 15334 (2015).
- ⁶¹S. M. Kashid *et al.*, *J. Phys. Chem. Lett.* **8**, 1604 (2017).
- ⁶²S. Park and M. D. Fayer, *Proc. Natl. Acad. Sci. U. S. A.* **104**, 16731 (2007).
- ⁶³C. Petersen, K.-J. Tielrooij, and H. J. Bakker, *J. Chem. Phys.* **130**, 214511 (2009).
- ⁶⁴W. S. Price, H. Ide, and Y. Arata, *J. Phys. Chem. A* **107**, 4784 (2003).
- ⁶⁵S. Roy and B. Bagchi, *J. Chem. Phys.* **139**, 034308 (2013).
- ⁶⁶T. Sato and R. Buchner, *J. Phys. Chem. A* **108**, 5007 (2004).
- ⁶⁷G. Stirnemann, P. Jungwirth, and D. Laage, *Proc. Natl. Acad. Sci. U. S. A.* **115**, E4953 (2018).
- ⁶⁸N. F. A. van der Vegt *et al.*, *Chem. Rev.* **116**, 7626 (2016).
- ⁶⁹D. S. Venables and C. A. Schmuttenmaer, *J. Chem. Phys.* **113**, 11222 (2000).
- ⁷⁰Q. Wei *et al.*, *J. Phys. Chem. B* **122**, 12131 (2018).
- ⁷¹L. R. Winther, J. Qvist, and B. Halle, *J. Phys. Chem. B* **116**, 9196 (2012).
- ⁷²D. B. Wong *et al.*, *J. Phys. Chem. B* **116**, 5479 (2012).
- ⁷³A. W. Omta *et al.*, *Science* **301**, 347 (2003).
- ⁷⁴X. Zhang *et al.*, *Mol. Phys.* **116**, 1014 (2018).
- ⁷⁵D. P. Geerke *et al.*, *J. Phys. Chem. B* **108**, 1436 (2004).
- ⁷⁶I. A. Borin and M. S. Skaf, *Chem. Phys. Lett.* **296**, 125 (1998).
- ⁷⁷A. K. Soper and A. Luzar, *J. Chem. Phys.* **97**, 1320 (1992).
- ⁷⁸A. K. Soper and A. Luzar, *J. Phys. Chem.* **100**, 1357 (1996).
- ⁷⁹I. Bakó, L. Pusztai, and L. Temleitner, *Sci. Rep.* **7**, 1073 (2017).
- ⁸⁰E. Guàrdia *et al.*, *J. Mol. Liq.* **117**, 63 (2005).
- ⁸¹M. Meot-Ner, *Chem. Rev.* **105**, 213 (2005).
- ⁸²S. Myneni *et al.*, *J. Phys.: Condens. Matter* **14**, L213 (2002).
- ⁸³A. V. Egorov, A. P. Lyubartsev, and A. Laaksonen, *J. Phys. Chem. B* **115**, 14572 (2011).
- ⁸⁴J. J. Towey and L. Dougan, *J. Phys. Chem. B* **116**, 1633 (2012).
- ⁸⁵L. Dougan *et al.*, *J. Chem. Phys.* **121**, 6456 (2004).
- ⁸⁶S. Banerjee, S. Roy, and B. Bagchi, *J. Phys. Chem. B* **114**, 12875 (2010).
- ⁸⁷R. Ghosh *et al.*, *J. Phys. Chem. B* **115**, 7612 (2011).
- ⁸⁸S. Roy *et al.*, *J. Phys. Chem. B* **115**, 685 (2011).
- ⁸⁹K.-I. Oh *et al.*, *Angew. Chem., Int. Ed. Engl.* **56**, 11375 (2017).
- ⁹⁰J. J. Towey, A. K. Soper, and L. Dougan, *J. Phys. Chem. B* **120**, 4439 (2016).
- ⁹¹P. G. Kusalik *et al.*, *J. Phys. Chem. B* **104**, 9533 (2000).
- ⁹²N. Nishi and K. Yamamoto, *J. Am. Chem. Soc.* **109**, 7353 (1987).
- ⁹³M. DeCamp *et al.*, *J. Phys. Chem. B* **109**, 11016 (2005).
- ⁹⁴E. Salamatova *et al.*, *J. Phys. Chem. A* **122**, 2468 (2018).
- ⁹⁵S. Lotze *et al.*, *J. Phys. Chem. B* **119**, 5228 (2015).
- ⁹⁶J. J. Gilijamse, A. J. Lock, and H. J. Bakker, *Proc. Natl. Acad. Sci. U. S. A.* **102**, 3202 (2005).
- ⁹⁷A. Perera *et al.*, *J. Mol. Liq.* **159**, 52 (2011).
- ⁹⁸F. A. Cotton and R. Francis, *J. Am. Chem. Soc.* **82**, 2986 (1960).
- ⁹⁹R. G. Pereyra, M. L. Asar, and M. A. Carignano, *Chem. Phys. Lett.* **507**, 240 (2011).
- ¹⁰⁰C. J. Wormald, *J. Chem. Thermodyn.* **34**, 1639 (2002).
- ¹⁰¹R. Gupta and G. N. Patey, *J. Phys. Chem. B* **115**, 15323 (2011).
- ¹⁰²O. Gereben and L. Pusztai, *Chem. Phys.* **496**, 1 (2017).
- ¹⁰³I. Bakó *et al.*, *Phys. Chem. Chem. Phys.* **15**, 15163 (2013).
- ¹⁰⁴S. Vishveshwara, K. V. Brinda, and N. Kannan, *J. Theor. Comput. Chem.* **1**, 187 (2012).
- ¹⁰⁵H. Lee *et al.*, *J. Phys. Chem. B* **119**, 14402 (2015).
- ¹⁰⁶H. Lee *et al.*, *J. Phys. Chem. A* **120**, 5874 (2016).
- ¹⁰⁷J. R. Errington and P. G. Debenedetti, *Nature* **409**, 318 (2001).
- ¹⁰⁸G. Ruocco, M. Sampoli, and R. Vallauri, *J. Chem. Phys.* **96**, 6167 (1992).
- ¹⁰⁹E. Duboué-Dijon and D. Laage, *J. Phys. Chem. B* **119**, 8406 (2015).
- ¹¹⁰J. Gujt *et al.*, *J. Mol. Liq.* **228**, 71 (2017).
- ¹¹¹E. Galicia-Andrés *et al.*, *J. Mol. Liq.* **209**, 586 (2015).
- ¹¹²K. P. Jensen and W. L. Jorgensen, *J. Chem. Theory Comput.* **2**, 1499 (2006).
- ¹¹³W. L. Jorgensen, "OPLS force fields," in *The Encyclopedia of Computational Chemistry* (John Wiley & Sons, New York, 1998).
- ¹¹⁴A. Vishnyakov, A. P. Lyubartsev, and A. Laaksonen, *J. Phys. Chem. A* **105**, 1702 (2001).
- ¹¹⁵P. Gómez-Álvarez, L. Romaní, and D. González-Salgado, *J. Chem. Phys.* **138**, 044509 (2013).
- ¹¹⁶E. Guàrdia, D. Laria, and J. Martí, *J. Phys. Chem. B* **110**, 6332 (2006).
- ¹¹⁷R. Chitra and P. E. Smith, *J. Chem. Phys.* **115**, 5521 (2001).

- ¹¹⁸M. Chalaris and J. Samios, "Computer simulation studies of the liquid mixtures water-dimethylsulfoxide using different effective potential models: Thermodynamic and transport properties," *J. Mol. Liquids* **98**, 401–411 (2002), available at <https://www.sciencedirect.com/science/article/abs/pii/S0167732201003440>.
- ¹¹⁹R. L. Mancera *et al.*, *Phys. Chem. Chem. Phys.* **6**, 94 (2004).
- ¹²⁰J.-C. Soetens and P. A. Bopp, *J. Phys. Chem. B* **119**, 8593 (2015).
- ¹²¹R. Halder and B. Jana, *J. Phys. Chem. B* **122**, 6801 (2018).
- ¹²²J. L. F. Abascal and C. Vega, *J. Chem. Phys.* **123**, 234505 (2005).
- ¹²³G. Palinkas, E. Hawlicka, and K. Heinzinger, *J. Phys. Chem.* **91**, 4334 (1987).
- ¹²⁴D. A. Tolmachev *et al.*, *J. Chem. Theory Comput.* **16**, 677 (2020).
- ¹²⁵J. Yoo and A. Aksimentiev, *J. Phys. Chem. Lett.* **3**, 45 (2012).
- ¹²⁶J. Yoo and A. Aksimentiev, *Phys. Chem. Chem. Phys.* **20**, 8432 (2018).
- ¹²⁷J. N. Onuchic, Z. Luthey-Schulten, and P. G. Wolynes, *Annu. Rev. Phys. Chem.* **48**, 545 (1997).
- ¹²⁸N. Ferguson and A. R. Fersht, *Curr. Opin. Struct. Biol.* **13**, 75 (2003).
- ¹²⁹J. N. Onuchic and P. G. Wolynes, *Curr. Opin. Struct. Biol.* **14**, 70 (2004).
- ¹³⁰B. Schuler and H. Hofmann, *Curr. Opin. Struct. Biol.* **23**, 36 (2013).
- ¹³¹M. Ediger and P. Harrowell, *J. Chem. Phys.* **137**, 080901 (2012).
- ¹³²U. Kaatz, R. Pottel, and M. Schaefer, *J. Phys. Chem.* **93**, 5623 (1989).
- ¹³³H. Frauenfelder, S. G. Sligar, and P. G. Wolynes, *Science* **254**, 1598 (1991).
- ¹³⁴S. Indra, B. Guchhait, and R. Biswas, *J. Chem. Phys.* **144**, 124506 (2016).
- ¹³⁵S. Ghosh *et al.*, *RSC Adv.* **4**, 14378 (2014).
- ¹³⁶A. F. Wallace *et al.*, *Science* **341**, 885 (2013).
- ¹³⁷K. J. Packer and D. J. Tomlinson, *Trans. Faraday Soc.* **67**, 1302 (1971).
- ¹³⁸C. Liang and T. L. C. Jansen, *J. Chem. Phys.* **135**, 114502 (2011).